Computational temporal ghost imaging

Fabrice Devaux[1*], Paul-Antoine Moreau[2], Séverine Denis[1] and Eric Lantz[1]
[1] *Institut FEMTO-ST,*
Département d'Optique P. M. Duffieux, UMR 6174 CNRS
Université Bourgogne Franche-Comté,
15b Avenue des Montboucons, 25030 Besançon - France
[2] *Centre for Quantum Photonics, H. H. Wills*
Physics Laboratory and Department of Electrical and Electronic Engineering
University of Bristol, Merchant Venturers Building,
Woodland Road, Bristol BS8 1UB, United Kingdom

We present a very simple device, inspired by computational ghost imaging, that allows the retrieval of a single non-reproducible, periodic or non-periodic, temporal signal. The reconstruction is performed by a single shot, spatially multiplexed, measurement of the spatial intensity correlations between computer-generated random images and the images modulated by the temporal signal, recorded and summed on a chip CMOS camera used with no temporal resolution.

I. INTRODUCTION

Exploitation of the statistical properties of classical or non classical light sources is the cause of fascinating new applications. For the two last decades, ghost imaging has emerged as a way to form images of an object with a Single Point Detector (SPD) that does not have spatial resolution. The initial works used the quantum nature of entanglement of a two-photons state, where photons of a pair are spatially correlated, to detect temporal coincidences [1]. While one of the photons passing through the object was detected by a photon counter with no spatial resolution, its twin photon was detected with spatial resolution by scanning the transverse plane with a single detector[1], or recently by an intensified charge-coupled device (ICCD) [2].

Later, ghost imaging exploiting the temporal correlations of the intensity fluctuations of pseudothermal light was proposed. With a two-detector setup [3], a ghost image of the object was obtained by correlating the pseudothermal field measured by a CCD with the intensity measured with a SPD. More recently, computational ghost imaging and ghost diffraction were performed with only one SPD [4, 5]: the object was illuminated by a pseudothermal light beam, generated with a Spatial Light Modulator (SLM) addressed with random phase masks. Then, the transmitted light was detected with the SPD. The image or the Fourier transform of the object was reconstructed by correlating the temporal fluctuations of the calculated field patterns with the measured intensities. With the same principle, ghost imaging with wavelength-multiplexing has been performed [6].

By taking into account space-time duality in optics, the extension of the results of spatial ghost imaging to the time domain has been investigated theoretically, numerically and recently experimentally either with a classical non-stationary light source [7, 8], bi-photon states [9], a chaotic laser [10] or a multimode laser source [11]. In all cases, the light emitted by the sources was split into two arms, called "reference" and "test" arms. While in the test arm the light was transmitted through a "time object" and detected with a slow SPD which can not properly resolve the time object, in the reference arm the light, that did not interact with the temporal object, was detected with a fast SPD. As for spatial ghost imaging, the temporal object was reconstructed by measuring the correlations of the temporal intensity fluctuations or the temporal coincidences between the two arms. In [11], measurements over several thousands copies of the temporal signal were necessary to retrieve an embedded binary signal with a good signal-to-noise ratio [12].

The extension of spatial ghost imaging to the time domain looks attractive for dynamic imaging of ultra-fast waveforms with high resolution. However, the currently proposed solutions require many realizations of the same temporal signal, limiting the current applications to the detection of synchronized and reproducible signals [12]. This is in contrast with spatial ghost imaging, where the object is unique, but multiplied in the time domain by a random modulation, different from one pixel to another, leading to multiplexing in this time domain. In the present paper we propose an original and completely different scheme which is the exact space-time transposition of computational ghost imaging [5]: a single shot acquisition of a non-reproducible time object is performed by multiplying it with computer-generated random images, ensuring spatial multiplexing of temporal intensity correlations before detection of the time integrated images with a camera that has no temporal resolution.

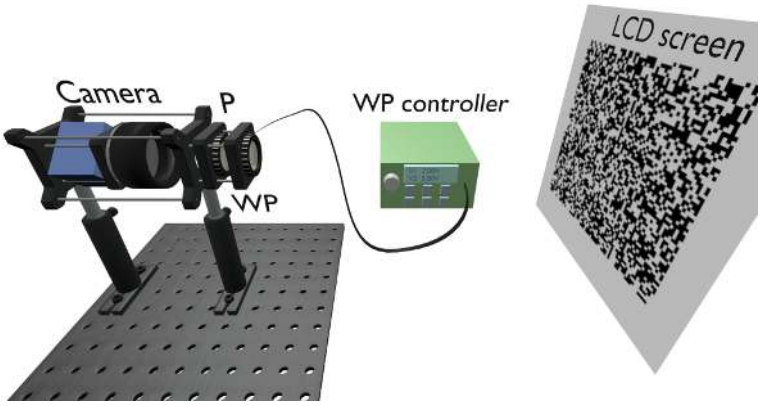

FIG. 1: Experimental setup : (P) linear polarizer (WP) liquid crystal variable wave plate. Images of random patterns displayed on a LCD screen are acquired with a CMOS camera. The transmission of the imaging system is modulated by a temporal signal that drives the WP placed in front of the polarizer.

II. RESULTS

Fig. 1 depicts the set-up. First, a stack of K independent random binary patterns X, with a large number of pixels, are generated and displayed on a LCD (Liquid Crystal Display) screen. In these binary patterns, a pixel takes the value 1 with probability p and the value 0 with probability $1-p$, hence verifies the statistical properties of a Bernouilli distribution ($\langle X \rangle = p$, $\sigma_X^2 = p(1-p)$). Images of the patterns are acquired with a compact CMOS USB2.0 camera (IDS UI-1640C, 1280×1024 pixels) on a 8 bits grey scale. Since the light emitted by the LCD screen is linearly polarised at 45°, the energy transmission of the imaging system can be linearly modulated by a temporal signal during the exposure time of the camera, by means of a liquid crystal variable wave plate (WP, Thorlabs LCC1113-A) placed before a linear polariser (P) in front of the camera objective.

At first, each pattern X_k of the stack (k denotes the rank of the pattern in the stack) is recorded individually with the same exposure time. The retardation of the WP and the direction of the polariser are adjusted to maximise the energy transmission of the imaging system, that will be considered in the following as a level of 100% ($T = 1$). Then, the mean and the variance of each image X'_k are measured. Since the displayed patterns are binary, the sharp edges of the original pixels are blurred in the recorded images because of the modulation transfer function (MTF) of the objective. Consequently, as the recorded images are encoded over 255 grey levels, they do no longer verify the initial statistical properties. Several experiments were conducted to optimize all the setup parameters (focus, numerical aperture and magnification of the objective, number of independent pixels in patterns, probability p) such as the statistical properties of intensity fluctuations in the recorded images are the closest of those of the computed patterns (see supplement).

In a second experiment, the patterns of the stack are displayed successively on the LCD screen, imaged with a transmission coefficient given by the driving temporal signal ($0 \leq T(t) \leq 1$), and summed on the camera during a long exposure time (5 to 10 s). In that case, the recorded image S corresponds to the time integrated image of the displayed patterns such as the level of a pixel S_{ij} of coordinates (i, j) is given by :

$$S_{ij} = \sum_{k=1}^{K} T(k) X'_{k,ij} \tag{1}$$

where $T(k)$ is the value of the transmission at the time when the k^{th} pattern is displayed. Fig. 2 shows a selected region of interest (ROI) in images of the displayed patterns. Fig. 2a corresponds to the image of a single pattern and Fig. 2b corresponds to the image of the time integrated patterns of the stack where a temporal object is embedded. Because the circular aperture of the WP limits the field of view of the imaging system and induces deterministic fluctuations for pixels close to the border, we selected the larger ROI of $N \times N$ pixels ($N = 700$) in images where the gray level of a lighted pixel is almost constant. In the subsequent calculations, residual covariances between images of two independent binary patterns, due to these deterministic intensity fluctuations, are removed by filtering numerically the recorded images. Because of the magnification of the imaging system, the image size of an independent pixel of the displayed patterns is larger than the size of a pixel of the camera. Then, the number of effective independent pixels in an image is smaller than the number of pixels in the selected ROI.

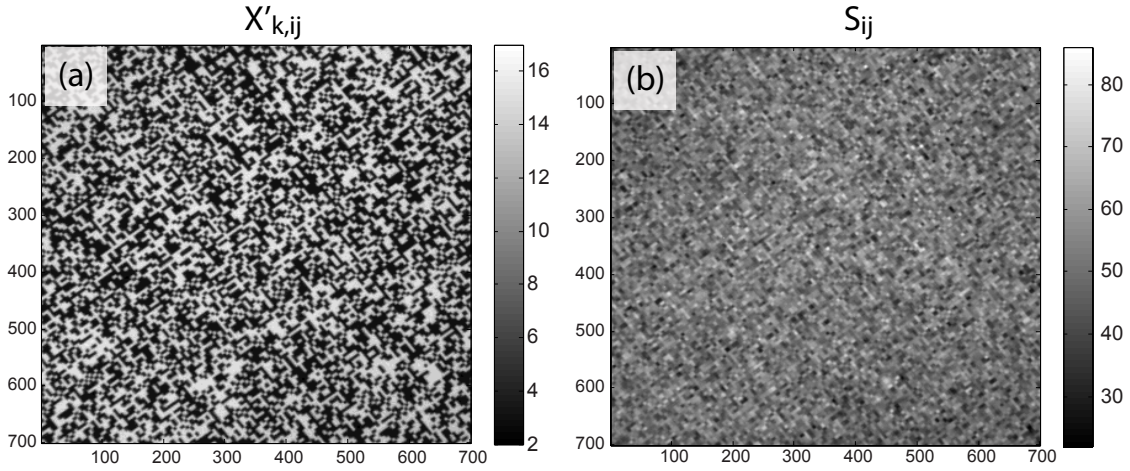

FIG. 2: (a) Image of a single random pattern where $p = 0.5$. (b) Image of the time integrated pattern's stack with a temporal object embedded. The measurements are performed inside a ROI of 700×700 pixels.

As for other methods of ghost imaging, the temporal signal is reconstructed by calculating the intensity correlations between the time integrated image S and the images X' of the K random patterns. The value of $T(k_0)$ at the "time" k_0 is estimated by (a hat means "estimator of"):

$$\hat{T}(k_0) = \frac{\gamma \sum_{i=1}^{N}\sum_{j=1}^{N}\left(S_{ij} - \overline{S}\right)\left(X'_{k_0,ij} - \overline{X}'_{k_0}\right)}{\sum_{i=1}^{N}\sum_{j=1}^{N}\left(X'_{k_0,ij} - \overline{X}'_{k_0}\right)^2} \tag{2}$$

where $\overline{S}$ and $\overline{X}'_{k_0}$ are the arithmetic mean levels of the related images. γ is a normalization coefficient corresponding to the ratio between the exposure time of the camera for the acquisition of the individual images X'_k and the display time of the random patterns during the acquisition of S. It can be shown (see supplement) that the noise in the measurement is minimized when $p = 0.5$. Then, the signal-to-noise ratio (SNR) is given by:

$$SNR[T(k_0)] = \frac{T(k_0)}{\sigma_{T(k_0)}} = \frac{N_{eff}T(k_0)}{\sqrt{\sum_{k=1,k\neq k_0}^{K} T^2(k)}} \geq \frac{N_{eff}}{\sqrt{K-1}}T(k_0) \tag{3}$$

where N^2_{eff} represents the total number of effective independent pixels in recorded images. With a ROI of 700×700 pixels, N^2_{eff} has been estimated as 153×153 independent pixels. Fig. 3 shows ghost images of different temporal signals (analogic or binary and periodic or non periodic). Each ghost image corresponds to a single shot measurement which is performed with images of 700×700 pixels (where $N_{eff} = 153$), the same stack of 20 random patterns (where $p = 0.5$) and a long camera exposure time between 6 s and 8 s. For periodic signals (figures 3a to Fig. 3c), the WP controller is driven in a linear regime by 0.5 Hz periodic signals with different shapes (square, sinus and ramp) which are depicted by the green curves (only phases of these curves are adusted to fit the experimental data represented by the blue stars). Error bars are deduced from the measured SNR. Voltage amplitude of these signals are fixed such as the transmission of the imaging system is in the range $0.4 \leq T(t) \leq 0.9$. These low and high transmission levels are depicted in Fig. 3a-c by the horizontal black dotted lines. Fig. 3d corresponds to the ghost image of a random binary word of 20 bits formed with a mechanical shutter ensuring $T = 0$ when closed, but $T < 1$ when open because opening is not synchronized with the display of the random patterns on the LCD screen. These results clearly show that our device is able to reconstruct, with a single shot measurement and with a very good accuracy, various temporal analogic or binary signals. We emphasize that thanks to the single shot measurement, our device allows non reproducible and non synchronizable signals to be recorded.

In order to measure the SNR, several single shot measurements were performed with the same experimental parameters and the WP controller driven by different continuous voltages such as the transmission coefficient is set as constants during the acquisition time of the ghost images (T =0.4, 0.9 and 1). The measured values are 0.38 ± 0.03, 0.90 ± 0.06 and 0.99 ± 0.08, respectively. Using Eq. 3, it corresponds to SNRs of 26 ± 8, 28 ± 6 and 26 ± 8, which are in rather good agreement with the theoretical SNR : $\frac{153}{\sqrt{19}} = 35$.

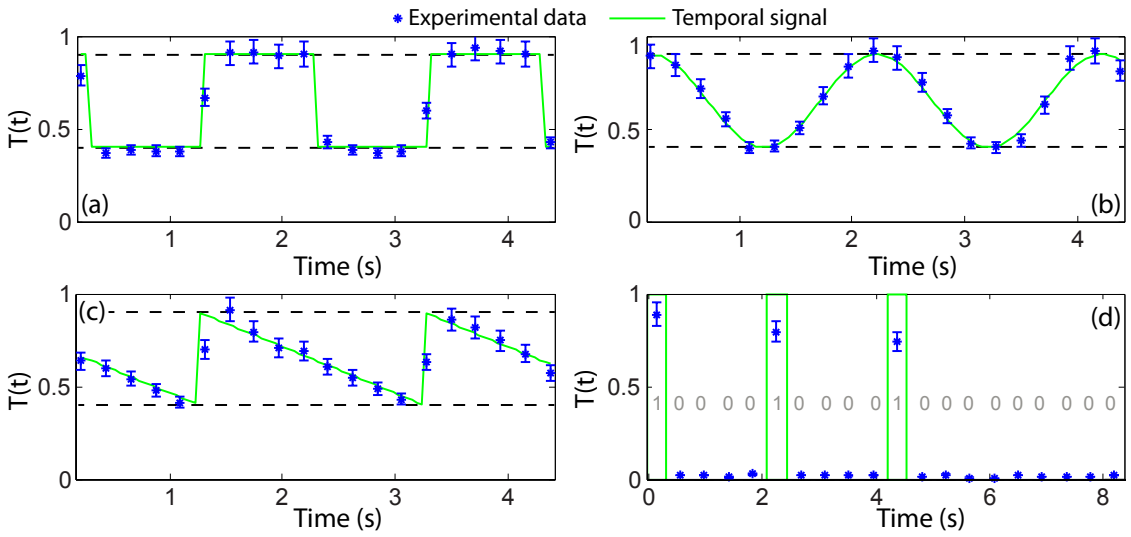

FIG. 3: Ghost images of different temporal signals. 3 kind of 0.5 Hz periodic signals: (a) square, (b) sinus, (c) ramp. (d) corresponds to the single shot measurement of a binary word of 20 bits. Each acquisition is performed with the same stack of 20 random patterns. Blue stars correspond to experimental data and the green curves show the original temporal signals. Error bars are deduced from the measured SNR. For periodic signals, horizontal black dotted lines show the effective amplitude of the transmission levels of the imaging system.

III. CONCLUSION

To summarize, these experiments represent the first demonstration of ghost imaging of a single, non-reproducible time object. They are performed by multiplying this object with computer-generated random images, ensuring the exact space-time transposition of computational ghost imaging. With a very simple device we were able to reconstruct with a very good accuracy different kinds of temporal signals. When compared to the recent experimental demonstration of temporal ghost imaging [11], the main advantage of our system consists in no need of multiple (thousands) synchronized copies of the temporal signal and the use of a single detector (the camera) that has no temporal resolution. In the present form of the set-up, its obvious drawback is the slowness which was imposed by the simple and low cost devices used to display the random patterns and to generate the temporal signals. The generation rate of random patterns with a large number of independent spatial modes can be easily increased by using either a fast digital micromirror device to display the random patterns up to tens of kHz [13] or spatial multiplexing of modulated light sources in multimode fibers to generate random patterns with a rate up to 100 MHz. More prospectively, exact space-time transposition of ghost imaging with thermal light [3] can be suggested where single shot acquisition of a temporal signal with sub-picosecond resolution could be obtained. First, patterns due to fast spatial fluctuations of a thermal-like light source are divided in two arms with a beam splitter. In the fist arm, spatial fluctuations of pattens are resolved with a high-speed photography device (a motion-picture camera with 4.4×10^{12} frames per second is reported in [14]), while in the second arm the same patterns are transmitted through a "time object" and integrated with a classical slow camera.

Authors contributions

F. Devaux and E. Lantz wrote the manuscript text. P.A. Moreau had the original idea of the experiment. F. Devaux designed the experimental setup and performed the experiments. E. Lantz developed the theoretical model. S. Denis participated to the experiments.

Funding

This work was supported by the Labex ACTION program (ANR-11-LABX-0001-01).

[1] T. B. Pittman, Y. H. Shih, D. V. Strekalov, and A. V. Sergienko, "Optical imaging by means of two-photon quantum entanglement," Phys. Rev. A **52**, R3429 (1995)
[2] P. A. Morris, R. S. Aspden, J. E. C. Bell, R. W. Boyd, and M. J. Padgett, "Imaging with a small number of photons," Nat. Commun. **6**, 5913 (2015)
[3] R. S. Bennink, S. J. Bentley, and R. W. Boyd, "Two-Photon coincidence imaging with a classical source," Phys. Rev. Lett. **89**, 113601 (2002)
[4] J. H. Shapiro, "Computational ghost imaging," Phys. Rev. A **78**, 061802 (2008)
[5] Y. Bromberg, O. Katz, and Y. Silberberg, "Ghost imaging with a single detector," Phys. Rev. A **79**, 053840 (2009)
[6] D.-J. Zhang, H.-G. Li, Q.-L. Zhao, S. Wang, H.-B. Wang, J. Xiong, and K. Wang, "Wavelength-multiplexing ghost imaging," Phys. Rev. A **92**, 013823 (2015)
[7] T. Shirai, T. Setälä, and A. T. Friberg, "Temporal ghost imaging with classical non-stationary pulsed light," JOSA B **27**, 2549 (2010)
[8] T. Setälä, T. Shirai, and A. T. Friberg, "Fractional Fourier transform in temporal ghost imaging with classical light," Phys. Rev. A **82**, 043813 (2010)
[9] K. Cho and J. Noh, "Temporal ghost imaging of a time object, dispersion cancelation, and nonlocal time lens with bi-photon state," Optics Communications **285**, 1275 (2012)
[10] Z. Chen, H. Li, Y. Li, J. Shi, and G. Zeng, "Temporal ghost imaging with a chaotic laser," Opt. Eng **5**, 076103 (2013)
[11] P. Ryczkowski, M. Barbier, A. T. Friberg, J. M. Dudley, and G. Genty, "Ghost imaging in the time domain," Nat Photon **10**, 167 (2016)
[12] D. Faccio, "Optical communications: Temporal ghost imaging," Nature Photonics **10**, 150 (2016)
[13] C. Gu, D. Zhang, Y. Chang, and S.-C. Chen, "Digital micromirror device-based ultrafast pulse shaping for femtosecond laser," Optics Letters **40**, 2870 (2015)
[14] K. Nakagawa, A. Iwasaki, Y. Oishi, R. Horisaki, A. Tsukamoto, A. Nakamura, K. Hirosawa, H. Liao, T. Ushida, K. Goda, et al., "Sequentially timed all-optical mapping photography (STAMP)," Nat. Photon. **8**, 695 (2014)